

## Transition to Chaos in Directional Solidification

K. Kassner,<sup>(1)</sup> C. Misbah,<sup>(2)</sup> and H. Müller-Krumbhaar<sup>(1)</sup>

<sup>(1)</sup>*Institut für Festkörperforschung des Forschungszentrums Jülich, W-5170 Jülich, Federal Republic of Germany*

<sup>(2)</sup>*Groupe de Physique des Solides, Universités Paris VI et VII,  
Centre National de la Recherche Scientifique, Place Jussieu, 75005 Paris, France*  
(Received 2 July 1991)

Interface dynamics are analyzed theoretically in the quasilocal regime of directional growth explored by experiments on liquid crystals. We discover “vacillating-breathing” (VB) modes. Upon variation of the growth speed the interface motion enters a chaotic regime via a quasiperiodicity scenario. Chaos occurs as a complex interplay between VB and parity-broken traveling modes. We suggest that the quasiperiodicity scenario should be generic for systems where these two modes coexist.

PACS numbers: 61.50.Cj, 05.70.Fh, 81.30.Fb, 68.70.+w

Directional growth of liquid crystals [1] and other one-dimensional pattern-forming systems [2–6] exhibit a myriad of dynamical phenomena. A particularly interesting example is the so-called “solitary” mode which has a broken-parity symmetry. This mode was first discovered by Simon, Bechhofer, and Libchaber [7]. The important idea that this mode is a localized inclusion of an asymmetric state resulting from a “secondary” bifurcation of the symmetric pattern was put forward by Coulet, Goldstein, and Gunaratne [8]. Later it was shown for eutectic systems [9] as well as for liquid crystals [10] that the “microscopic” models do support parity-broken solutions extending along, and moving transversely to, the whole front. More recently [11], an approach to the experimental generation of a parity-broken state filling (virtually) the whole front was proposed. This suggestion has been confirmed by recent experiments [6].

Another seemingly generic feature pertains to the so-called “optical modes” [1], where the cell width oscillates in phase opposition with its neighbors. Below we will adopt the denomination “vacillating-breathing” (VB) mode for reasons that will become clear. In an interesting paper, Coulet and Iooss [12] use symmetry arguments to classify ten generic secondary instabilities which include the VB mode. It remains to be shown, however, which of these modes are realized within a specific “microscopic” model. It is also of great importance to investigate the subsequent development of possible instabilities. In particular, one expects any tertiary instability to lead to complex dynamics and eventually to chaos. It is the aim of this Letter to deal with these questions. By focusing on the liquid-crystal experiments [1], we find, besides parity-broken modes, that there exists a secondary instability in the form of a VB mode. With increasing growth speed the VB mode undergoes an instability (tertiary instability) that mixes the VB and the parity-broken (PB) modes. The interface behaves as a quasiperiodic system. At larger speeds the interface motion enters a chaotic regime. So far this transition occurs via a direct destruction of the invariant 2-torus in phase space on which the quasiperiodic motion takes place.

There are many experimental situations [1,3–6] where VB and PB modes coexist. We suggest that quasiperiodicity generically precedes chaos for those systems.

In general the equation that governs the front dynamics involves nonlocal and retarded interactions, which causes difficulties [13] for both analytical and numerical investigations. Fortunately, many of the interesting phenomena [1] occur at large growth speed where the diffusion length  $l=2D/V$  ( $V$  is the growth speed and  $D$  the diffusion constant) is small as compared to the wavelength  $\lambda$  of the pattern. We then expect the dynamics to be quasilocal. A local asymptotic equation (close to the planar-front restabilization) has been derived for the one-sided model of growth by Brattkus and Davis [14]. More recently a derivation of a local evolution equation appropriate for the small diffusion lengths in liquid crystals has been given [15]. That equation reads, for the interface profile  $\zeta(x,t)$ ,

$$3\zeta_{xxxx} - 4\zeta_{xxt} + \zeta_{tt} + 8\zeta_{xx} + 8l\bar{\tau}^{-1}\zeta \\ = 4\zeta_x\zeta_{xt} + 2\zeta_{xx}\zeta_t - 4(\zeta_x^2)_{xx} - 2(\zeta_x^3)_x + 2\zeta_{xx}^2. \quad (1)$$

It contains up to fourth-order derivatives in the space variable  $x$  normal to the growth direction and up to second-order time derivatives. Lengths and time have been reduced by  $l$  and  $l^2/D$ , respectively. Note that  $x$  and  $t$  are “slow” variables [15] renormalized by the appropriate small parameter which expresses the *locality* of the dynamics. The only parameter that remains in our equation,  $l\bar{\tau}^{-1}$ , is proportional to  $G/V$ , where  $G$  is the applied thermal gradient; the proportionality coefficient depends on material properties only and its precise definition is unimportant for our purposes. Equation (1) obviously admits a planar-front solution ( $\zeta=0$ ), the linear stability of which yields the dispersion relation  $\omega^2 + 4\omega q^2 + 3q^4 - 8q^2 + 8l\bar{\tau}^{-1} = 0$ , where  $\omega$  is the growth rate and  $q$  the wave number of the perturbation. The critical conditions for the onset of the planar-front instability ( $\omega = \partial\omega/\partial q = 0$ ) provide the critical values  $l\bar{\tau}_c^{-1} = 2/3$  and  $q_c = 2/\sqrt{3}$ . The planar front is unstable for  $l\bar{\tau}^{-1} < l\bar{\tau}_c^{-1}$ . Figure 1 shows the neutral curve in the

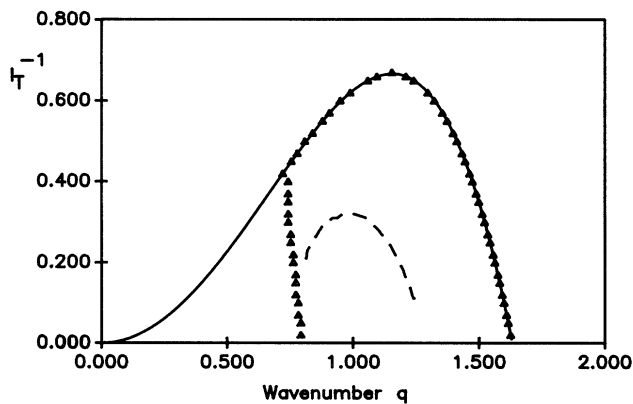


FIG. 1. The solid line represents the neutral curve. The triangles delimit the domain of existence of steady and symmetric solutions. The dashed line is the boundary below which oscillatory instabilities occur (see text).

$(l_T^{-1}, q)$  plane, inside which the planar solution is unstable. The first step of our investigation consists of determining periodic reflection-symmetric steady solutions of Eq. (1). The domain of existence of this continuous family of solutions is delimited by the triangles in Fig. 1. Solutions exist up to the neutral curve for large wave numbers, while for small wave numbers they run into a *fold* singularity and merge with solutions having  $2q$  as a basic wave number. This feature was met in other contexts [16]. At wave numbers slightly above the fold singularity solutions with a broken parity appear as a forward bifurcation. This feature is very similar to that encountered in eutectic systems [11], but will not constitute a central point of this Letter [17].

Having defined the domain of existence of steady solutions we are in a position to study the *secondary* instabilities (we use the term *primary* instability with the planar front as reference). We look for solutions of Eq. (1) in the form  $\zeta = \zeta_{0q}(x) + \zeta_1(x, t)$ , where  $\zeta_{0q}(x)$  is the steady solution parametrized by the wave number  $q$ . Inserting this into Eq. (1) and neglecting all but linear terms we obtain a partial differential equation (of second order in time) with periodic coefficients (stemming from  $\zeta_{0q}$ ) for the deviation  $\zeta_1$ . Setting  $\zeta_1 = e^{\Omega t} f(x)$  and  $\zeta_{1t} = e^{\Omega t} g(x)$  in that equation, it transforms into an eigenvalue problem of the form  $Lu = \Omega u$ , where  $u$  is a vector defined by  $u = (f, g)$  and  $L$  is a  $2 \times 2$  linear operator which commutes with the translation operator  $T_\lambda$  ( $\lambda = 2\pi/q$ ) due to the periodicity of the basic solution. The Floquet-Bloch theorem then states that the general solution can be written as  $u(x) = e^{iQx} \hat{u}(x)$ , where  $\hat{u}(x + \lambda) = \hat{u}(x)$ , and  $Q$  is a real constant. In a reduced-zone representation, it suffices to restrict  $Q$  to the first Brillouin zone, defined here as  $0 \leq Q \leq q$ . Our next step is to expand  $\hat{u}$  in Fourier series. This results in a  $2N \times 2N$  matrix equation for the Fourier coefficients, where  $N$  represents the number of Fourier modes. For all the cases treated here,

twenty modes apparently were more than sufficient. The condition that the determinant should vanish leads to  $2N$  branches  $\Omega_{i,q}(Q)$  ( $i = 1, \dots, 2N$ ) for a given  $q$ . As we are interested in the onset of instability we simply need to locate the value of  $q$  (for a given  $l_T^{-1}$ ) for which at least one branch has a positive real part. Close to  $l_T^{-1}$  we find, as expected, that the most dangerous fluctuations are those leading to the Eckhaus instability, confirming the result obtained from phase dynamics [15]. As  $l_T^{-1}$  decreases (which means as  $V$  increases at fixed thermal gradient  $G$  as in usual experiments), there appear short-wavelength oscillatory instabilities. More precisely, for  $l_T^{-1} < 0.3$  we find an oscillatory instability which occurs at  $Q = q/2$  for a wide range of the basic wave number (see Fig. 1). This instability leads to spatial *period doubling*. At the onset ( $l_T^{-1} \approx 0.3$ ), the frequency of oscillations,  $\text{Im}(\Omega)$ , changes slightly with  $q$  and is approximately on the order of  $\text{Im}(\omega) \sim 0.9$ . Typically in liquid-crystal experiments [1] the time scale is  $l^2/D \sim 10^{-3} - 10^{-2}$  s (for  $V \sim 100 \mu\text{m/s}$ ). The small parameter that enters the asymptotic theory is of the order of  $\epsilon \sim 0.1$  (which is typically the order of the inverse Péclet number). Since the physical time scales [15] as  $\epsilon^2$ , the period of oscillation is typically in the range of a second, which is a usual value in experiments [1].

In order to understand the long-time behavior of the growing instabilities and possible tertiary instabilities we must look for a dynamical solution of the full evolution equation (1). We have performed a numerical integration of Eq. (1). The spatial derivatives are evaluated in Fourier space. This (spectral) procedure is accurate for higher-order spatial derivatives. The resulting dynamical system is solved by means of Gear's backward difference method [18]. We restrict ourselves here to systems with an aspect ratio between 2 and 4. For  $l_T^{-1} > 0.3$  the code reproduces well the steady solutions computed by standard Newton-Raphson or shooting schemes. We have made calculations just beyond the onset of the oscillatory instability found from the linear stability analysis described above. Figure 2 shows the evolution of the interface for  $l_T^{-1} = 0.29$  and  $q = 0.9$  after transients have disappeared. As could be expected from the linear analysis the interface shows a spatial period-doubling oscillatory instability. The cell width oscillates in phase opposition with its neighbors (vacillation). Note also that the top of the cell oscillates in a *breathing* fashion. We adopt for this mode the denomination *vacillating-breathing* mode. The period of oscillation is, within a few percent, as predicted by the linear theory. This mode of growth has been observed in various systems [1,3,4,6,19]. Note that this mode is symmetric with respect to reflection about the growth axis.

An important question is whether the VB mode may itself undergo an instability, and if so what type of dynamics would then emerge. By decreasing  $l_T^{-1}$  down to a value slightly above 0.28 we find that the dynamics are

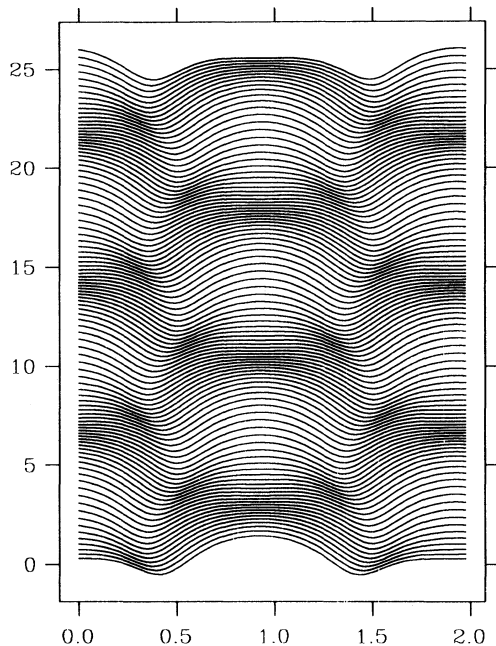


FIG. 2. Interface dynamics exhibiting a VB mode. The vertical coordinate represents time.

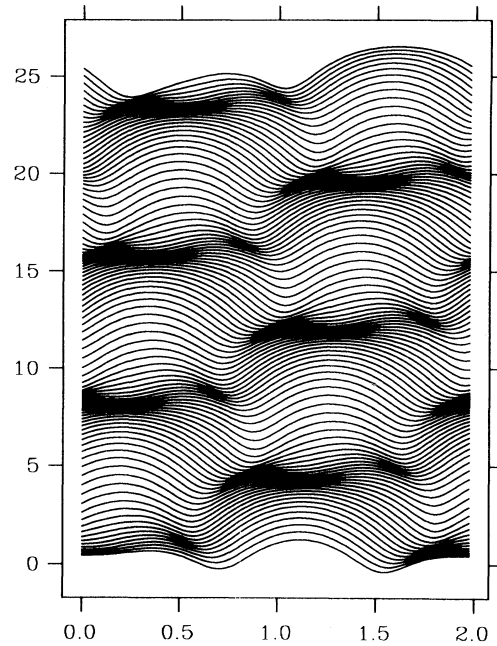


FIG. 3. Interface dynamics showing a mixture of VB and PB modes.

similar to what is shown in Fig. 2, but the effect of the second (temporal) harmonic increases continuously. At  $l_T^{-1} \approx 0.28$  the limit cycle (associated with the VB mode) undergoes an instability characterized by a loss of the overall parity symmetry. As a consequence, the pattern drifts sideways, while the VB mode subsists. Figure 3 shows the interface evolution. Now each point on the interface is subject to (i) the VB oscillation (with a frequency denoted by  $f_1$ ) and (ii) an oscillation resulting from the drift, with a frequency  $f_2$ . Indeed, the Fourier spectrum reveals the presence of sharp peaks at  $f_1$  and  $f_2$  (with  $f_1 > f_2$ ). All the other peaks are either higher harmonics or combinations of the form  $||mf_1 + nf_2||$ , with  $m, n$  integers. The motion is quasiperiodic. For  $l_T^{-1} = 0.27$  the Poincaré map (Fig. 4) is almost continuous, thus indicating that the trajectories densely cover the invariant 2-torus in phase space. The ratio  $f_1/f_2 \sim 6.2$ . For  $0.28 > l_T^{-1} > 0.25$  the motion remains quasiperiodic, without any appearance of mode locking. Below  $l_T^{-1} = 0.25$  the Fourier spectrum becomes denser; the mode with the smallest frequency ( $f_2$ ) shows the beginning of a subharmonic cascade (already at  $l_T^{-1} = 0.26$ ) which is a precursor of the transition to chaos. At  $l_T^{-1} = 0.24$  the invariant 2-torus has broken up in favor of a *strange attractor*, as shown in Fig. 5. This breakdown is preceded by the appearance of low-frequency lines in the Fourier spectrum. The spectrum at  $l_T^{-1} = 0.24$  forms a continuum. We will give a detailed picture in an extended publication, where we will deal with further questions, in particular those regarding scaling laws close to the onset of

chaos [20,21].

In the prechaotic and chaotic regimes the interface shows temporal irregularity, while the spatial order is preserved. The interface morphology consists, for various regimes, essentially of only two spatial modes  $a_1(t)e^{iqx}$  and  $a_2(t)e^{i2qx}$ , while all the higher harmonics are linearly damped and therefore slaved to these. This means that the front dynamics can be mapped, in Fourier space, onto that of a purely dynamical system with only two (active) modes. As Eq. (1) is in fact of second order in time, the

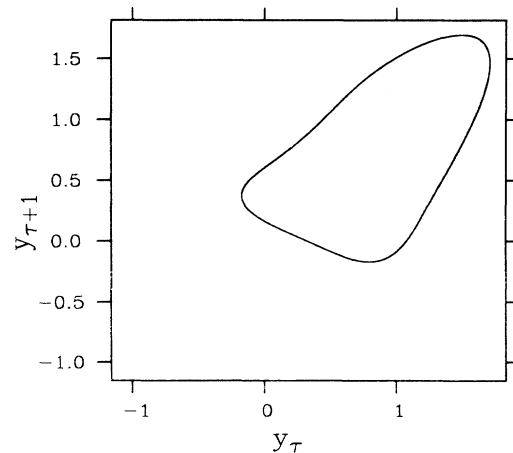


FIG. 4. The Poincaré map at  $l_T^{-1} = 0.27$ . The motion is quasiperiodic.

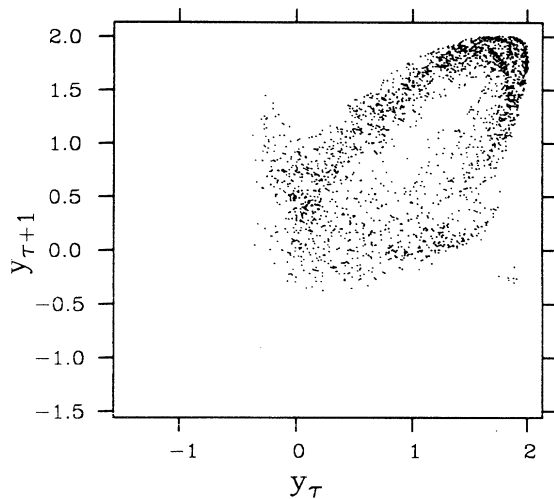


FIG. 5. The Poincaré map at  $l_T^{-1}=0.24$  showing the destruction of the 2-torus in favor of a strange attractor.

“active dimension” of phase space, for pure amplitude dynamics, is equal to 4. This is largely sufficient to topologically allow the creation of a strange attractor. This question is currently under investigation. Note that here we considered systems with small aspect ratio only. We would like in the future to study for larger systems the possible transition to spatiotemporal chaos.

In summary, we have given the first theoretical communication for the onset of chaos in directional growth of liquid crystals. As the growth speed increases, the initially steady interface undergoes, at a critical growth speed, a continuous Hopf bifurcation, which manifests itself as a (spatial) period-doubling oscillation and is characterized by a mixture of vacillation and breathing. This VB mode is completely symmetric with respect to the growth axis. On further increase of the growth speed a tertiary instability intervenes which is parity breaking. As a result the pattern drifts. The interface dynamics then consist of a complex mixture of VB and PB modes. The system behavior is quasiperiodic. At a critical velocity the 2-torus associated with quasiperiodicity breaks up in favor of a strange attractor. There have been recently many suspicions, in various growth experiments and similar phenomena [1,3,4,6], that the irregular pattern is a trace of a chaotic motion. As there are many situations where VB and PB modes coexist, we believe that the transition to chaos involving quasiperiodicity should be generic. This

Letter is also a suggestion for experimental investigations with the aim to study quantitatively the possible routes to chaos.

We are grateful to S. Thomae for valuable discussions.

- 
- [1] J. M. Flesselles, A. J. Simon, and A. Libchaber, “Dynamics of One-Dimensional Interfaces: An Experimentalist’s View” (to be published).
  - [2] G. Faivre, S. de Cheveigné, C. Guthmann, and P. Kurowski, *Europhys. Lett.* **9**, 779 (1989).
  - [3] M. Rabaud, S. Michalland, and Y. Couder, *Phys. Rev. Lett.* **64**, 184 (1990).
  - [4] S. de Cheveigné and C. Guthmann, “Interface Dynamics and Anisotropy Effects in Directional Solidification” (to be published).
  - [5] J. T. C. Lee and R. A. Brown, “Spatiotemporal Chaos Near the Onset of Cellular Growth During Thin-Film Solidification of a Binary Alloy” (to be published).
  - [6] G. Faivre, C. Guthmann, and J. Mergy (private communication).
  - [7] A. J. Simon, J. Bechhofer, and A. Libchaber, *Phys. Rev. Lett.* **61**, 2574 (1988).
  - [8] P. Coulet, R. Goldstein, and G. H. Gunaratne, *Phys. Rev. Lett.* **63**, 1954 (1989).
  - [9] K. Kassner and C. Misbah, *Phys. Rev. Lett.* **65**, 1458 (1990); *Phys. Rev. Lett.* **66**, 522 (E) (1991).
  - [10] H. Levine and W. Rappel, *Phys. Rev. A* **42**, 7475 (1990).
  - [11] K. Kassner and C. Misbah (to be published).
  - [12] P. Coulet and G. Iooss, *Phys. Rev. Lett.* **64**, 866 (1990).
  - [13] Note that numerical integration of the integral equation has so far been performed within the quasistationary approximation only: Y. Saito, C. Misbah, and H. Müller-Krumbhaar, *Phys. Rev. Lett.* **63**, 2377 (1989).
  - [14] K. Brattkus and S. H. Davis, *Phys. Rev. B* **38**, 11462 (1988).
  - [15] A. Ghazali and C. Misbah “Phase Instability in Directional Solidification” (to be published).
  - [16] L. H. Ungar and R. A. Brown, *Phys. Rev. B* **29**, 1367 (1984); **31**, 5923 (1985); **31**, 5931 (1985).
  - [17] Some of these results are discussed in Ref. [15].
  - [18] C. W. Gear, *Numerical Initial-Value Problems in Ordinary Differential Equations* (Prentice-Hall, Englewood Cliffs, NJ, 1971).
  - [19] M. Zimmermann, A. Karma, and M. Carrard, *Phys. Rev. B* **42**, 833 (1990), and references therein.
  - [20] M. J. Feigenbaum, L. P. Kadanoff, and S. J. Shenker, *Physica (Amsterdam)* **5D**, 370 (1982).
  - [21] S. Ostlund, D. Rand, J. Sethna, and E. Siggia, *Physica (Amsterdam)* **8D**, 303 (1983).